Available online at www.sciencedirect.com

ScienceDirect

Ceramics International 40 (2014) 3165–3170

CERAMICS INTERNATIONAL

www.elsevier.com/locate/ceramint

# Modification of glass ionomer cement by incorporating hydroxyapatite-silica nano-powder composite: Sol–gel synthesis and characterization

Rayees Ahmad Shiekh*, Ismail Ab Rahman, Sam'an Malik Masudi, Norhayati Luddin

*School of Dental Sciences, Universiti Sains Malaysia, 16150 Kubang Kerian, Kelantan, Malaysia*

Received 3 August 2013; received in revised form 28 September 2013; accepted 28 September 2013
Available online 17 October 2013

**Abstract**

A nanohydroxyapatite–silica powder was synthesized using an ethanol based sol–gel technique. The synthesized powder was incorporated into commercial glass ionomer powder (Fuji II GC) and characterized using FTIR, $^{29}$Si CP/MAS NMR, EDX and XRD spectroscopy. $^{29}$Si CP/MAS NMR results showed the presence of higher degree of cross-linking of silyl species between silica and GIC, which makes the Nano-HA–Silica–GIC composite much stronger. High-resolution transmission electron microscopy (TEM) and scanning electron microscopy (TEM) was employed to investigate the morphology of the synthesized powder. Results revealed that higher content of nanosilica produced a denser and stronger GIC. Thus, the application of nanohydroxyapatite–silica–GIC with improved properties are envisioned to be of great clinical importance, especially in stress bearing areas.


*Keywords:* Glass ionomer cement; Silica–nanohydroxyapatite; Sol–gel technique; Characterization

## 1. Introduction

Glass ionomer cement (GIC) first developed by Wilson and Kent in the late 1960s is widely used in clinical dentistry [1–4]. GIC, classified as acid–base reaction cement, consists of an aqueous solution of polyacrylic acid and an acid-decomposable fluoro-aluminosilicate glass powder [5–9]. The increasing interest for GIC is due to the biocompatibility and ability of the material for regeneration of hard tissues including bones and tooth structure. Other advantages of GIC include good adhesion to the tooth or bone, releases fluoride that acts as an anti cariogenic, and requires minimal cavity preparation.

In spite of these favorable properties, GIC exhibits some limitations as dental restorative materials, mainly due to their susceptibility to dehydration, poor physical properties as a result of high solubility and slow setting rate, by which the latter further lead to poor mechanical properties, namely low fracture strength and toughness, low wear resistance [10]. A number of attempts have been made to overcome the problems, which include the application of different fillers, such as silver-cermets, stainless steel powders, carbon and alumino-silicate fibers and, incorporation of hydroxyapatite into glass-polyalkenoate [6,7,11,12]. Hydroxyapatite ($Ca_{10}(PO_4)_6(OH)_2$, HA) has an excellent biological behavior and has played a vital role in orthopedics applications due to its favorable osteo-conductive and bioactive properties [8,9,13,14]. HA behaves as such due to its similar chemical composition and crystal structure to apatite in the human skeletal system and is therefore suitable for bone substitution and reconstruction [15,16]. GIC with the incorporation of HA have been found to improve the biocompatibility and physical properties [17]. In recent years, HA has shown promising advantages in restorative dentistry, including its biocompatibility, hardness similar to that of natural tooth and intrinsic radiopaque response [18,19]. Although it is a naturally occurring mineral form of calcium apatite, technological advances have enabled nanosized HA to be prepared by many different methodologies, for instances, wet chemical preparation, sol–gel synthesis, co-precipitation, etc. [20]. Glass ionomer cements (GICs) are a class of bioactive cements that bond directly to bone. A new bioactive hydroxyapatite (HA)/silica-filled GIC composite were developed to improve the biocompatibility and bioactivity of the GICs with the

*Corresponding author. Tel.: +60 9 7675818; fax: +60 9 7642026.
*E-mail address:* rayeeschem@gmail.com (R. Ahmad Shiekh).

0272-8842/$ - see front matter © 2013 Elsevier Ltd and Techna Group S.r.l. All rights reserved.
http://dx.doi.org/10.1016/j.ceramint.2013.09.127

surrounding bone and connective tissues. A number of researchers have attempted to evaluate the effect of the addition of HA powders GIC on mechanical properties. The effect on addition of HA on the compressive strength, diametral tensile strength [21], flexural strength [19], toughness, bonding and fluoride-release properties of GIC has been reported [22]. Recently, we have reported the methods of producing nano-HA–silica composite by the one-pot sol–gel technique [23], and in addition the nanocomposite has increased the hardness of the GIC by ~73% [23]. It is envisaged that the nanosilica particles may fill the void between the hexagonal shaped HA particles, and form denser and stronger nanohydroxyapatite-silica nanocomposite powder. The present study aims to evaluate the chemical interaction between filler and GIC, using different characterization techniques including FTIR, $^{29}$Si CP/MAS NMR, EDX and XRD spectroscopy. In addition, the morphological-nature of nano crystals was investigated using Transmisson Electron Microscopy (TEM) and Scanning Electron Microscopy (SEM), to provide more evidence to ascertain our previous findings.

## 2. Materials and methods

Nanohydroxyapatite–silica–GIC (nano-HA–silica–GIC) was synthesized following a reported protocol [22]. A stiochiometric amount of 7.408 g of calcium hydroxide ( > 98%, RM Chemicals) was mixed and stirred in 100 ml of distilled water to produce a suspension. Phosphoric acid (4.104 ml > 99%, Aldrich) was then added drop wise to the suspension and pH was adjusted to the range of 11–12 using ammonia. The suspension was then stirred for 48 h. 5 ml of TEOS (99%, Fluka) diluted in 10 ml of ethanol was added drop wise after 12 h of stirring. The sol was centrifuged, dried using a freeze dryer and calcined at 600 and 700 °C for 1 h. Pure nanosilica was prepared following a procedure reported elsewhere [24], meanwhile pure HA was prepared by following the above procedure without addition of TEOS.

Nano-HA–silica was mixed with a commercial GIC (Fuji IX GP, GC International Japan). The nano-Ha–silica–GIC cement was made by spatulation of the powder mixture into the liquid at a powder/liquid ratio of 1:1 and mixed according to the manufacturer's instructions. Following that, the cement was covered with moisten gauze and left for 24 h to enable complete setting reaction.

Morphology of the synthesized materials was studied using Scanning Electron Microscopy (SEM, Leo Supra 50VP) and Transmission electron microscopy (TEM) and the images were taken using a Philips CM 12 system. $^{29}$Si NMR was obtained using a cross-polarization magic angle spinning (CP/MAS) solid state nuclear magnetic resonance (NMR, Bruker AV 400WB). FTIR spectra were recorded using a Perkin-Elmer 2000 FT-IR spectrometer. The samples were analyzed qualitatively by XRD analysis. The scanning was done from 10° to 60° at a rate of 0.02°/min (Bruker, D2, PHASER) using Cu-Kα radiation generated at 30 kV and 10 mA. The crystalline phases were determined from a comparison of the registered patterns with the International Center for Diffraction Data (ICDD) powder diffraction file (PDF).

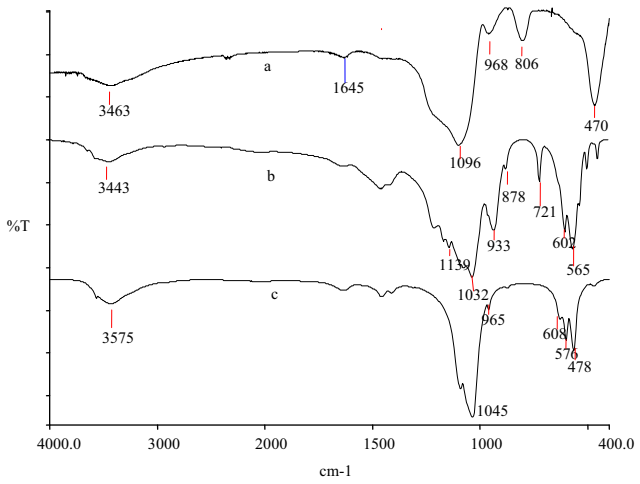


Fig. 1. FTIR spectra of (a) silica, (b) HA-Silica and (c) HA.

## 3. Results and discussion

### 3.1. FTIR analysis

Fig. 1(b) shows the FTIR spectrum of nano-HA–Silica which is the combination of silica (a) and hyroxyapatite (c), according to the observed stretching frequencies (968 $cm^{-1}$, 878 $cm^{-1}$, 608 $cm^{-1}$, 576 $cm^{-1}$ and 565 $cm^{-1}$) etc. and the similarity of the FTIR spectra of the investigated samples, the possible formation of crystalline hydroxyapatite–silica-nanocomposite by sol–gel synthesis route could be suggested [23].

### 3.2. Solid-state NMR analysis

Valuable structural information about the silica and nano-HA–silica–GIC can be obtained by means of Solid-state NMR spectroscopy. In solid state samples, due to the limited motion, strong dipolar–dipolar and chemical shift anisotropy interactions has occurred due to the limited motion. The line broadening effects can be canceled using magic angle spinning (MAS) technique. Other problems which arise in solid-state NMR spectroscopy related to the strong hetero nuclear interactions and the existence of very long spin-lattice relaxation times $T_1$ of the order of minutes to hours are solved in the cross polarization (CP) technique [25].

Silane functionality according to the used silane type, bonding chemistry and the different surface species that result can be distinguished by $^{29}$Si CP/MAS NMR measurements. So, the monofunctional species (M) appear in the region from 13 to −1 ppm, difunctional species (Dn) from −7 to −20 ppm, trifunctional species (Tn) from −49 to −66 ppm and signal from the starting silica from –91 to –110 ppm (Fig. 2).

A higher degree of cross-linking of silyl species and/or of oxygen neighbors has led to an upfield shift in NMR spectra. Fig. 3 presents the $^{29}$Si CP/MAS NMR spectra of silica and nano-HA–silica–GIC. The spectrum of silica contains the

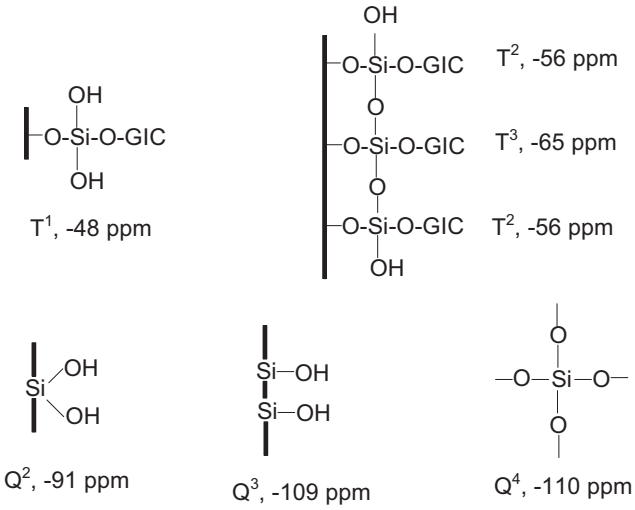


Fig. 2. Nomenclature and chemical shifts of some silyl species.

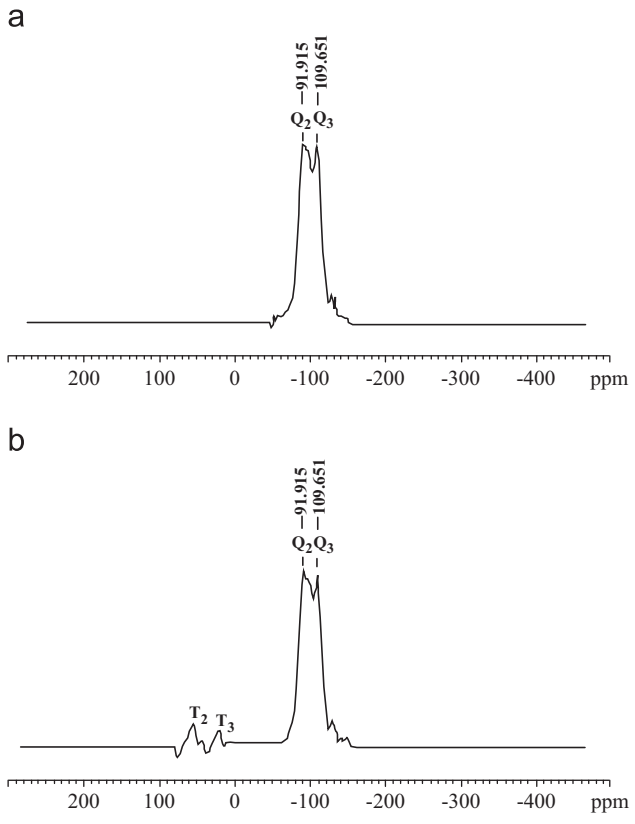


Fig. 3. $^{29}$Si CP/MAS NMR spectra (a) Unmodified silica and (b) Chemically modified material HA–Silica–GIC.

signals assigned to the Q species, $Q^2$ (–91 ppm) and $Q^3$ (–109 ppm) showed a high amount of free –OH groups on the surface. In the spectrum of nano-HA–silica–GIC the signals of trifunctional species (Tn) assigned to $T^2$ (–56 ppm) and $T^3$ (–65 ppm) groups were observed. The shoulder at –91 ppm was assigned to $Q^2$-groups which were still available on the surface. The signal of the $Q^3$-groups has a high intensity. This spectrum indicates a high cross linking on the modified surface and a lower surface coverage. The high field shifted signal at 10 ppm belongs to the C–1 closest to the surface, in the neighborhood of the silicon [26].

### 3.3. X-ray diffraction (XRD) and EDX analysis

An XRD pattern of sol–gel prepared HA–silica composite and silica powder that was sintered at 600 °C is shown in Fig. 4(a and b) respectively. A single XRD peaks present in Fig. 4(a) at 20°–22° 2$\theta$ (scanning range) corresponds to the presence of silica while as in Fig. 4(b) these peaks were shifted to 26°–27° 2$\theta$ and a new sharp peak observed at 32°–33° 2$\theta$ that corresponds to the presence of hydroxyapatite. The presence of these peaks elucidates the formation of HA–silica composite. The sintering temperature plays an important role in the formation of HA–silica composite. As the sintering temperature is increased to 600 to 700 °C, several peaks of XRD pattern which belongs to the HA–silica powder become more distinct and also the width of the peaks become narrower, which suggest an increase in the degree of powder crystallinity. It has been reported that HA decomposes within the temperature range of 600–800 °C, and decomposition temperature strongly depends to the characteristics and synthetic technique of the HA powder [27]. In order to obtain pure HA–silica in this study, the sintering temperature selected was 600 °C. The XRD patterns of the powders post heat treatment also reveals that no other calcium phosphate phase are present in the powders.

EDX results in Fig. 5 shows that the main elements present in the HA–Silica composite powder are calcium, phosphorus, carbon, oxygen and silicon. Hence the formation of HA–silica composite by the presence of silicon in the EDX fig is confirmed.

### 3.4. Characterization of nano powders

#### 3.4.1. TEM and SEM evaluation

Comparative morphologies of nanohydroxyapatite, nanohydroxyapatite–silica and nano hydroxyapatite–silica in GIC matrix prepared by the sol–gel technique, as observed under TEM are shown in Fig. 6. The images clearly show that the elongated rod shaped structure is indeed hydroxyapatite (HA) (Fig. 6a) and from the Fig. 6b apart from the rod shaped HA structures, spherical powder like structures embedded within elongated HA are the silica particles [28,29]. These images reveal that all the powders are in nanosize range with the mean size of the elongated HA and silica was approximately 95 nm and 25 nm respectively. As a result, we can say that the morphology of the hydroxyapatite–silica nanocomposite powder consists of a mixture of spherical silica particles embedded within the voids of elongated hydroxyapatite.

Fig. 6c shows the morphology of hydroxyapatite–silica nanocomposite powder completely embedded in glass Ionomer cement (GIC) matrix. By increasing the concentration of nanosilica, the voids of HA were filled completely resulting in denser cement and thus a stronger GIC.

A representative SEM micrograph of nanohydroxyapatite–silica nanocomposite powder (Fig. 7(a)), clearly reveals that nanocomposite powder is a mixture of elongated rod shaped

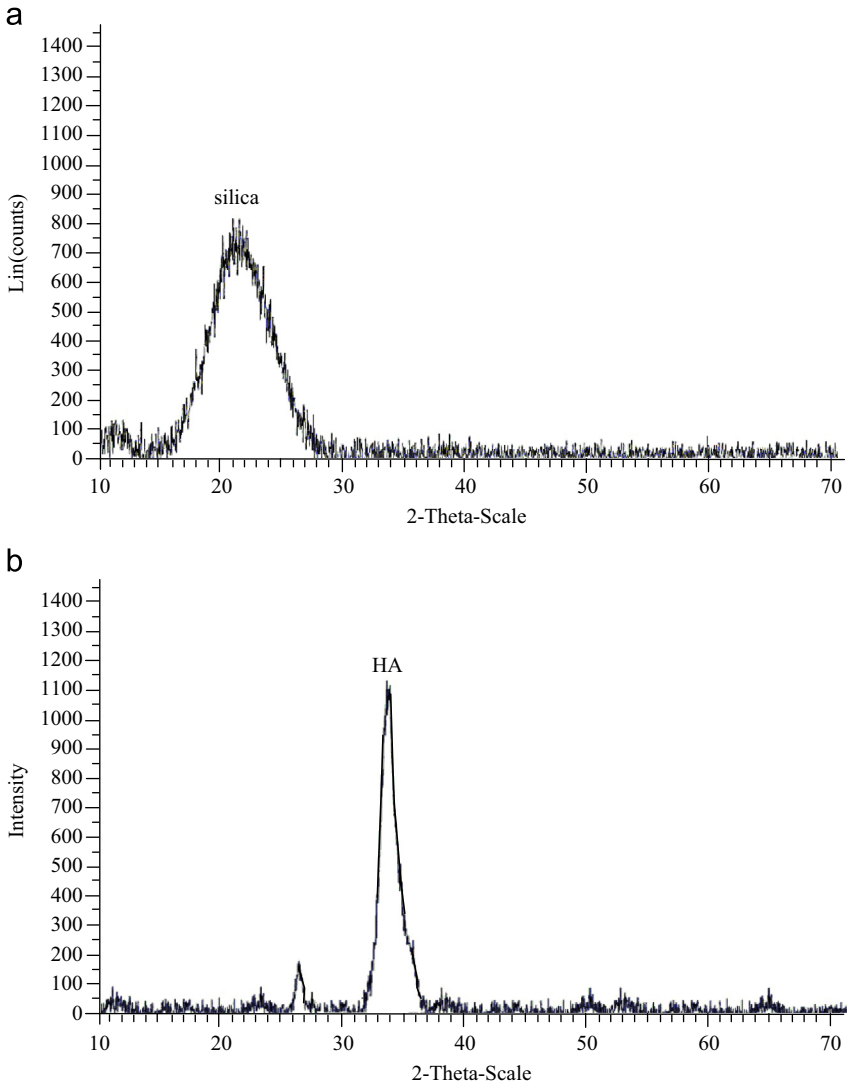


Fig. 4. X-ray diffraction (XRD) pattern of: (a) Unmodified silica and (b) Chemically modified material HA–Silica–GIC.

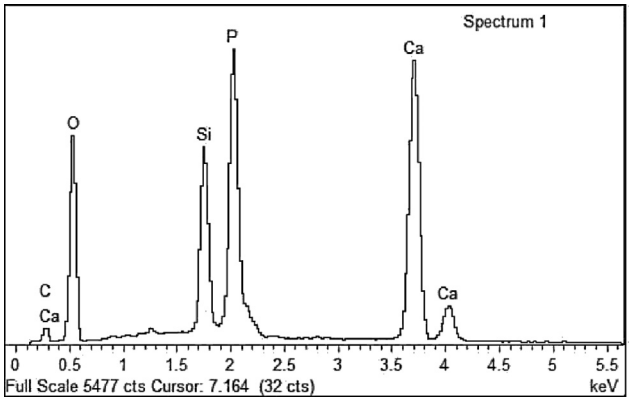


Fig. 5. EDX spectrum of HA–silica composite powder.

like structures which is hydroxyapatite and a spherical powder shaped structure which is silica. It also confirms that silica has occupied the voids present between HA structures and form a denser and stronger nanohydroxyapatite–silica nanocomposite powder.

Fig. 7(b) clearly shows the microstructure of the composite and distribution of various components, packing density of silica particle size of fillers within matrix of GIC, under dot mapping SEM.

## 4. Conclusions

This paper investigates the detailed structural analysis of HA–silica nanocomposite powder, synthesized successfully by the sol–gel method. SEM, TEM, FTIR and $^{29}$Si CP/MAS NMR tools were used to elucidate the atomic scale characterization. $^{29}$Si CP/MAS NMR clearly shows the presence of higher degree of cross-linking of silyl species between silica and GIC, which makes the Nano-HA–Silica–GIC composite much stronger. The phase purity and information of various chemical species has been characterized by XRD and EDX techniques. The nano crystalline nature has been ascertained by XRD and high resolution SEM micrographs. TEM and SEM characterization revealed that the morphology of HA–silica nanocomposite was a mixture of spherical silica particles embedded within

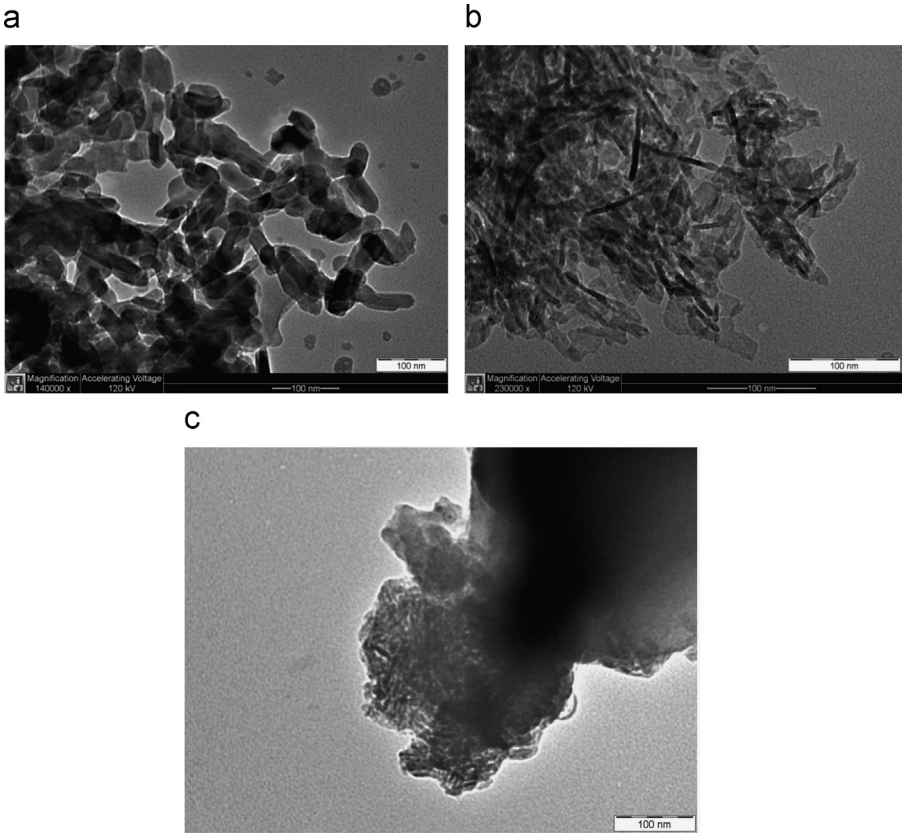


Fig. 6. TEM micrographs of (a) nanosilica and (b) nanohydroxyapatite (c) Nano hydroxyapatite–silica in GIC matrix.

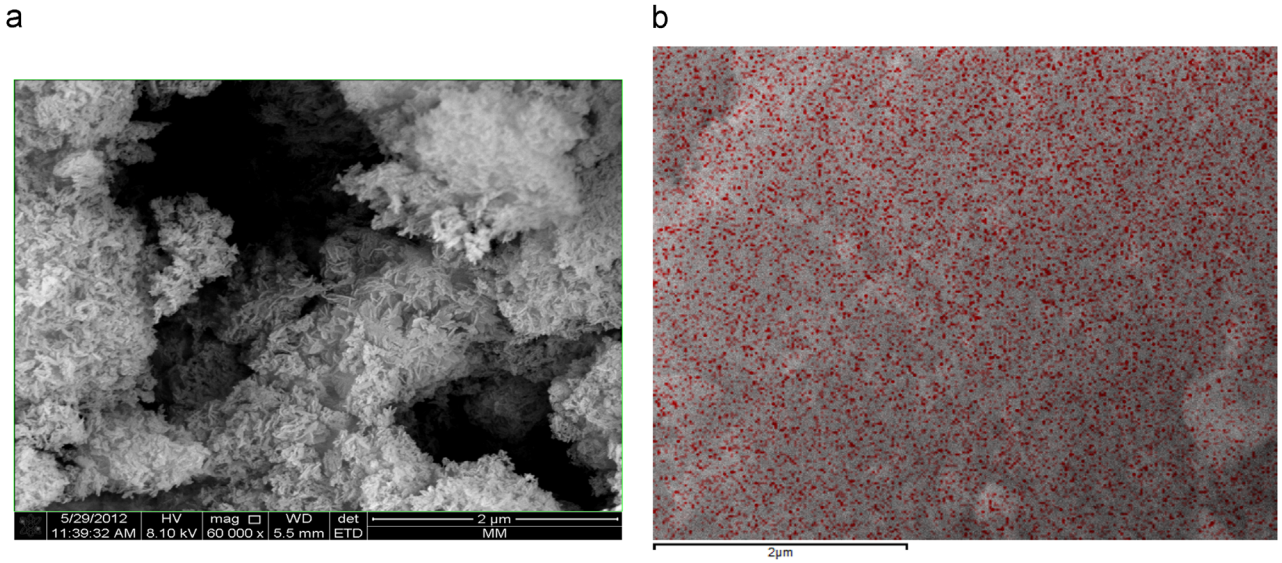


Fig. 7. (a) SEM micrographs of HA–$SiO_2$ nanocomposite and (b) Dot mapping SEM micrograph of HA-$SiO_2$ nanocomposite.

elongated HA and also confirms the HA–silica nanocomposite powder is completely embedded in GIC matrix. It can be concluded that higher content of nanosilica, results in denser cement and produces a stronger GIC. Application of HA–silica–GIC with improved properties might lead to extended clinical indications, especially in stress bearing areas.

## Acknowledgment

Financial support of this research work, sponsored by the Malaysian Ministry of Higher Education under fundamental Research Grant scheme (FRGS/203/PPSG/6171138) is highly acknowledged.

## References


[1] A.D. Wilson, B.E. Kent, A new translucent cement for dentistry, the glass ionomer cement, Br. Dent. J. 132 (1972) 133–135.

[2] J.W. McLean, G.J. in: Mount (Ed.), An atlas of glass-ionomer cements—a clinician's guide, Martin Dunitz Ltd., London, 1990.

[3] R. Maijer, D.C. Smith, A comparison between zinc phosphates and glass ionomer cements in orthodontics, Am. J. Orthodont. Dentofac. Orthoped. 93 (1998) 273–279.

[4] A.D. Wilson, Secondary reactions in glass-ionomer cements, J. Mater. Sci. Lett. 15 (1996) 275–276.

[5] J.W. Nicholson, Chemistry of glass-ionomer cements: a review, Biomaterials 19 (1998) 485–494.

[6] W. Zollner, C. Rudel, Glass ionomers: the next generation, in: P. C. Hunt, (Ed.), Proceedings of the Philadelphia International Symposium in Dentistry (1994) 57–60.

[7] L.M. Jonck, C.J. Grobbelaar, H. Strating, The biocompatibility of glass-ionomer cement in joint replacement—bulk testing, Clin. Mater. 4 (1989) 85–107.

[8] R.T. Ramsden, R.C.T. Herdman, R.H. Lye, Ionomeric bone cement in otoneurological surgery, J. Laryngol. Otol. 106 (1992) 949–953.

[9] J.W. Nicholson, J.H. Braybrook, E.A. Wasson, The biocompatibility of glass-poly(alkenoate) (glass-ionomer) cements: a review, J. Biomater. Sci. Polym. Edn. 2 (4) (1991) 277–285.

[10] G.J. Mount, An atlas of glass-ionomer cement: A clinician's guide, 2nd ed., Martin Dunitz, London, 1994.

[11] S.K. Sidhu, T.F. Watson, Resin-modified glass ionomer materials, Am. J. Dent. 8 (1) (1995) 59–66.

[12] F. Kawano, M. Kon, M. Kobayashi, K. Miyai, Reinforcement effect of short glass on strength of fibers with $CaO–P_2O_5–SiO_2–Al_2O_3$ glass-ionomer cement, J. Dent. 29 (5) (2001) 377–380.

[13] H.H.K. Xu, F.C. Eichmiller, J.M. Antonucci, G.E. Schumacher, L.K. Ives, Dental resin composites containing ceramic whiskers and precured glass ionomer particles, Dent. Mater. 16 (5) (2000) 356–363.

[14] R.R. Rao, H.N. Roopo, T.S. Kannan, Solid state synthesis and thermal stability of HAP-b-TCP composite ceramic powders, J. Mater. Sci. Mater. Med. 8 (1997) 511–518.

[15] A.C. Tas, F. Korkusuz, M. Timucin, N. Akkas, An investigation of the chemical synthesis and high-temperature sintering behavior of calcium hydroxyapatite (HA) and tricalcium phosphate (TCP) bioceramics, J. Mater. Sci. Mater. Med. 8 (1997) 91–96.

[16] E.O. Martz, V.K. Goel, M.H. Pope, J.B. Park, Materials and design of spinal implants—a review, J. Biomed. Mater. Res. 38 (1997) 267–288.

[17] J.W. Nicholson, S.J. Hawkins, J.E. Smith, The incorporation of hydroxyapatite into glass-polyalkenote (glass-ionomer) cements: a preliminary study, J. Mater. Sci. Mater. Med. 4 (1993) 418–421.

[18] R.W. Arcis, A. López-Macipe, M. Toledano, E. Osorio, R. Rodríguez-Clemente, J. Murtra, M.A. Fanovich, C.D. Pascual, Mechanical properties of visible light-cured resins reinforced with hydroxyapatite for dental restoration, J. Dent. Mater. 18 (1) (2002) 49–57.

[19] K. Arita, M.E. Lucas, M. Nishino, The effect of adding hydroxyapatite on the flexural strength of glass ionomer cement, J. Dent. Mater. 22 (2) (2003) 126–136.

[20] S.V. Dorozhkin, Review of nanosized and nanocrystalline calcium orthophosphates, Acta Biomater. 6 (3) (2010) 715–734.

[21] J.W. Nicholson, S.J. Hawkins, J.E. Smith, The incorporation of hydroxyapatite into glass polyalkenoate (glass-ionomer) cements: a preliminary study, J. Mater. Sci. Mater. Med. 4 (4) (1993) 418–421.

[22] M.E. Lucas, K. Arita, M. Nishino, Toughness, bonding and fluoride-release properties of hydroxyapatite-added glass ionomer cement, Biomaterialia 24 (21) (2003) 3787–3794.

[23] I.A. Rahman, S.M. Masudi, N. Luddin, R.A. Shiekh, One-pot synthesis of hydroxyapatite-silica nano-powder composite for hardness enhancement of glass Ionomer cement (GIC), Bull. Mater. Sci. (2013) (BOMS-D-12-00448).

[24] I.A. Rahman, P. Vejaykumaran, C.S. Sipaut, J. Ismail, M. Abu Bakar, R. Adnan, C.K. Chee, An optimized sol–gel synthesis of primary equivalent silica particles, Colloidal Surf. A: Physicochem. Eng. Aspects 294 (2007) 102–110.

[25] K. Albert, E. Bayer, Characterization of bonded phases by solid-state nmr-spectroscopy, J. Chromatogr. 544 (1991) 345–370.

[26] P. Vejeyakumaran, I.A. Rahman, C.S. Sipaut, J. Ismail., C.K. Chee, J. Colloid Interface Sci. 328 (2008) 81–91.

[27] A. J. Ruys, K. A. Zeigler, O. C. Standard, A. Brandwood, B. K. Milthorpe, C. C. Sorrell, Hydoxyapatite sintered phenomena, in: M. J. Branster (Ed.), Ceramics: Adding the value, Proceeding for the international ceramic conference, AUSTCERAM-92, CSIRO, Melbourne, 2, (1992) 605.

[28] M. Jafarzadeh, I.A. Rahman, C.S. Sipaut, Synthesis of silica nanoparticles by modified sol-gel process: The effect of mixing modes of the reactants and drying techniques, J. Sol–Gel Sci. Technol. 50 (2009) 328–336.

[29] R.N. Panda, M.F. Hsieh, R.J. Chung, T.S. Chin, FTIR, XRD, SEM and solid state NMR investigations of carbonate-containing hydroxyapatite nano-particles synthesized by hydroxide-gel technique, J. Phys. Chem. Solids 64 (2) (2003) 193–199.